AJVR

AVMA

CT attenuation of the medial coronoid process is reduced in dogs with medial coronoid disease but independent of arthroscopic disease severity

William J. Humphreys, BVSc[1]; Katie Wilder, BVSc[2]; Rob Pettitt, BVSc[1]; Eithne J. Comerford, PhD[1,3]; Thomas W. Maddox, PhD[1,3]*

[1]Small Animal Teaching Hospital, School of Veterinary Science, Institute of Veterinary and Ecological Sciences, University of Liverpool, Leahurst Campus, Neston, UK
[2]Avon Lodge Veterinary Group, Salisbury, UK
[3]Department of Musculoskeletal and Ageing Sciences, Institute of Life Course and Medical Sciences, University of Liverpool, Liverpool, UK

*Corresponding author: Dr. Maddox (thomas.maddox@liverpool.ac.uk)

https://doi.org/10.2460/ajvr.21.10.0171

OBJECTIVE
To compare the attenuation of the medial coronoid process (MCP) in dogs with and without arthroscopically confirmed evidence of medial coronoid disease (MCD).

ANIMALS
The database at our institution was searched for cases with thoracic limb lameness, diagnosed with MCD by arthroscopic examination that had CT as part of their investigation and compared with a control group of elbow joints from cadavers euthanized for reasons unrelated to MCD. A total of 84 elbow joints were included that met these criteria.

PROCEDURES
Following CT, a standardized measurement of the MCP was obtained from apex to base and the mean attenuation, SD, and total area were recorded. A comparative measurement was obtained from the proximal radial cortex at the level of the nutrient foramen. Elbow joint arthroscopy was carried out using standard portals, and the modified Outerbridge score was (MOS) used to score elbow joint cartilage. Descriptive and inferential statistics were carried out using MLwiN and R.

RESULTS
Attenuation of the MCP was reduced in dogs with MCD compared with those with no MCD ($P < .002$). No significant differences were observed in the attenuation between categories of severity (MOS). There was good inter- and intraobserver agreement between measurements (intraclass correlation coefficient = 0.89 and 0.95, respectively).

CLINICAL RELEVANCE
MCP attenuation is reduced in dogs with MCD compared with dogs with no evidence of MCD. This finding may be a useful tool for early detection of MCD, but there is no relationship with arthroscopic lesion severity.

Canine elbow dysplasia (CED) is an umbrella term first defined by the International Elbow Working Group.[1] It encompasses multiple developmental anomalies of the canine cubital joint, including ununited anconeal process, humeral osteochondrosis, articular cartilage injury, elbow incongruity, and fragmentation of the medial coronoid process (FMCP).[2–6] CED results in chronic thoracic limb lameness in young, large breed dogs secondary to irreversible arthritis and is a significant cause of morbidity in this population.[3,4,7–9] It is also reported in some chondrodystrophic small-breed dogs.[4,10]

FMCP is the most common heritable form of CED.[11,12] Recently, this term has been superseded by medial coronoid disease (MCD)—a broader term that incorporates the wide spectrum of cartilage pathology associated with the medial coronoid process (MCP), of which fragmentation is the end stage.[13] The etiopathogenesis of MCD has been widely debated, with incongruity of the elbow joint postulated to be the most likely cause. Humeroulnar incongruity and trochlear notch deformity,[14] radioulnar incongruity,[4,15] and primary rotational incongruity[16,17] have all been suggested as possible inciting causes, with or without concurrent defects in endochondral ossification.[18] Regardless of the aberrant anatomic conformation, a supraphysiologic load is placed on the MCP, causing subchondral microfractures and

ultimately grossly evident fissures, and these features have been observed histologically[19] and by using micro-CT.[20]

The diagnosis of MCD remains challenging, with direct examination of the medial compartment via arthroscopy (alone or in combination with additional imaging) remaining the gold standard.[11] Radiography has been the standard modality used for diagnosis, grading, and screening for CED and MCD, but interpretation is confounded by the superimposition of the complex three-dimensional anatomy of the elbow joint.[2] It is rare to see a discrete osteochondral fragment with MCD; therefore, radiographic diagnosis of MCD, and FMCP, is based on the detection of secondary signs. These include proximal anconeal osteophytosis, proximal radial osteophytosis, subchondral sclerosis of the semilunar notch, and alterations in the radiographic silhouette and lucency of the MCP alongside exclusion of other primary causes such as ununited anconeal process and osteochondrosis.[2]

Consequently, other advanced imaging modalities have been used in the detection of MCD, both qualitatively and quantitatively. CT has been widely investigated, alleviating issues with superimposition and permitting multiplanar reconstruction of acquired images.[2,21] In a recent study,[22] CT was reported to have a sensitivity of 100% and specificity of 93% compared with arthroscopy for the assessment of MCD, and it also permits quantification of incongruency.[23–26] In parallel, MRI permits imaging in multiple planes with exquisite soft tissue detail, with superior contrast resolution available from combinations of multiple sequences.[26] MRI is more sensitive than radiography for detection of an abnormal MCP,[27] and a recent report highlighted a statistically significant correlation between articular cartilage lesions observed with MRI and modified Outerbridge score (MOS) at arthroscopic examination.[28] However, its clinical applications remain limited by its cost, prolonged anesthetic time, and limited availability.

Quantitative assessment of the density of the MCP has been investigated in vivo, with dual-energy x-ray absorptiometry and CT using both osteoabsorptiometry (CTOAM) and Hounsfield units to infer bone mineral density (BMD).[5,6,8,29] The Hounsfield unit is a standardized linear attenuation coefficient scale defining air as –1,000 and purified water as 0, with greater values correlating to increased BMD and vice versa.[29] A recent topographic study[6] quantifying the attenuation of the MCP, suggested a caudolateral load transfer in elbow joints affected with MCD, and a lower overall BMD. The potential utility of CT to provide further insights into the underlying pathophysiology of CED, and as a noninvasive semiquantitative screening tool for subclinical disease, should not be underestimated.

The aim of this study was to assess the attenuation of the MCP in dogs with and without MCD. The null hypothesis is that there would be no overall difference between the attenuation of the radial cortex and the MCP in dogs with and without MCD.

Material and Methods

Case recruitment

For assessment of the attenuation of the MCP in a population of dogs with confirmed MCD, the clinical records database at our institution was searched for cases that presented with thoracic limb lameness subsequently diagnosed with MCD by arthroscopic examination. Cases were included if they had a CT examination of one or both elbow joints and subsequent arthroscopic confirmation of MCD in the same elbow joint or joints. The full signalment of each patient was recorded.

In the control population, both elbow joints were scanned from a population of canine cadavers euthanized for reasons unrelated to thoracic limb disease. Elbow joints were scanned within 24 to 48 hours of euthanasia and stored at 4 °C until required. Arthroscopic examination was performed immediately following CT scanning.

Ethical approval was received from the University of Liverpool Veterinary Ethics Committee under reference RETH000553.

Imaging and arthroscopic examination

Computed tomography

CT was performed routinely for both cases and control animals using the standard protocol at our institution. An 80-slice CT scanner (Toshiba Aquilon, Toshiba Medical Systems) was used to scan each elbow joint, with the patient positioned in sternal recumbency and the elbow joint in extension. The scan field of view was adjusted to extend from the proximal third of the radius to the distal third of the humerus of the elbow joint of interest. Typical acquisition parameters are included for reference—helical scan mode: pitch, 0.625; 50 to 70 mA; 100 to 120 kV; slice thickness, 0.5 to 1.0 mm; reconstruction kernel: sharp bone and soft tissue).

CT scan analysis

All images were reviewed retrospectively by a general practice veterinarian (observer 1) and an European College of Veterinary Diagnostic Imaging (ECVDI) resident in diagnostic imaging (observer 2) under similar guidance from a board-certified radiologist. Multiplanar reformatting was performed using proprietary image viewing software (Osirix 11.0, Pixmeo) for image analysis using the bone reconstruction and routine window width and length.[30] Reviewers were blinded to the arthroscopic findings at the time of review. The attenuation (measured in Hounsfield units) of the caudoproximal radial cortex was measured using the polygon tool at the level at which the nutrient foramen perforates the ulnar cortex **(Figure 1)**. The attenuation of the MCP was also measured using the polygon tool to outline a line parallel to but not including the medullary cavity of the ulna and around the MCP from apex to base on a single slice (Figure 1). Where gross fragmentation of the MCP was evident, any fragments were not included within the measurement area. The total area, mean attenuation, and SD were recorded at each

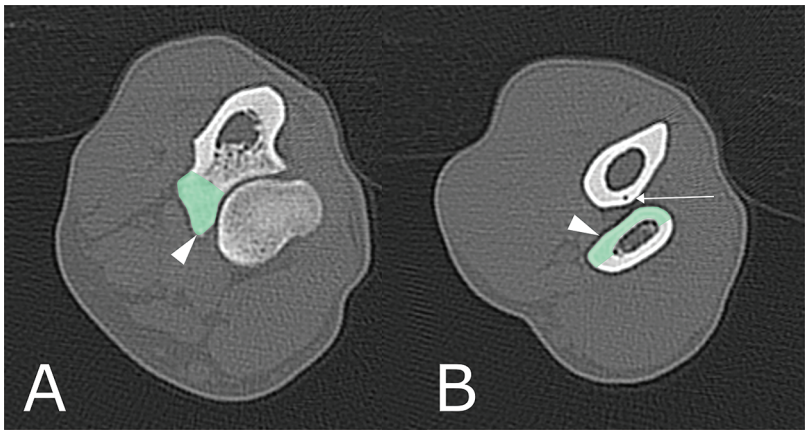

Figure 1—A representative example of axial CT images (bone reconstruction) delineating regions (arrowheads) around the medial coronoid process (A) from apex to base and the proximal radial cortex (B) at the level of the nutrient foramen (arrow) used to quantify attenuation.

Table 1—Table outlining the Modified Outerbridge score used to classify medial coronoid lesions arthroscopically

Modified Outerbridge score (MOS)	Description of gross cartilage quality
0	Normal
1	Chondromalacia (assessed by use of an arthroscopic probe)
2	Partial thickness fibrillation
3	Deep fibrillation
4	Full-thickness cartilage loss (exposure of the subchondral bone)
5	Subchondral bone eburnation

site. One measurement at each site was recorded by observer 1, and 2 separate, and identical, measurements were recorded by observer 2. The arithmetic mean was calculated for the measurements across all observers and this value used for data analyses.

Arthroscopic examination

A standard arthroscopic examination of each elbow joint was performed in cases and control animals to examine the medial and lateral compartments of the elbow joint using medial portals as described by Beale et al.[31]

Arthroscopic examination was carried out by a board-certified surgeon (European College of Veterinary Surgeons [ECVS] or Royal College of Veterinary Surgeons [RCVS]) or a resident under the supervision of a board-certified surgeon to provide direct observation of the MCP and confirmation of disease status. A modified Outerbridge cartilage grading system (MOS) **(Table 1)** was used to classify the pathology of the articular cartilage in the medial compartment of the elbow joint. The findings were recorded in a surgical report by the attending clinician immediately after examination.

Where pathological arthroscopic lesions were identified in presumptively normal cadaveric animals, these animals were regrouped and included in the dogs with confirmed MCD for statistical analysis **(Figure 2)**.

Statistical analysis

Statistical analysis was carried out using R (version 4.0.2, R Foundation for Statistical Computing) and MLwiN (version 3.02, Centre for Multilevel Modelling, University of Bristol).

Each elbow joint was treated as an individual case for statistical analysis and was classified into a group based on the MCD status as determined by the MOS, recorded immediately after arthroscopic examination. Elbow joints were initially categorized as normal (MOS = 0) or abnormal (MOS > 0). The abnormal group was then subclassified by MOS grade for further statistical analysis. As only a single case was assessed with an MOS = 4, this case was included with cases graded with an MOS of 3 to create a category of MOS of 3 or more for final analysis (Figure 2).

Primary outcome variables for data analysis between groups were mean attenuation (measured in Hounsfield units) and SD (measured in Hounsfield units) of the MCP and proximal radial cortex (PRC), and an arbitrary unitless value calculated to normalize the attenuation of the MCP to that of the PRC, calculated as MCP/PRC (measured in Hounsfield units/Hounsfield units).

Descriptive analysis was performed for all variables. The data were assessed for normality using visual histogram assessment, Q-Q plot analysis, and the Shapiro-Wilk test for normality. Based on the normality assessment, parametric testing was deemed appropriate. A paired *t* test was used to assess for significant differences between the attenuation of the PRC and MCP across all grading categories.

Interobserver variability between observer 1 and observer 2. and intraobserver variability for observer 2 was assessed by calculation of the intraclass correlation coefficient ([ICC] including 95% CIs) using a 2-way random effects model, as described by Koo and Li.[32]

Given the clustering of the data attributed to treating each elbow joint as a single case, multilevel linear regression analysis was deemed appropriate for assessing the relationships between the primary outcome variables, arthroscopic grade (MOS), and, ultimately, MCD status. Within-dog clustering of elbow joints was accounted for as a random intercept term in these 2-level models. $P < .05$ was considered significant in all analyses.

Results

Group 1: cases with arthroscopic evidence of MCD (MOS > 0)

A total of 42 dogs were identified from our institution with CT examination of one or both elbow joints,

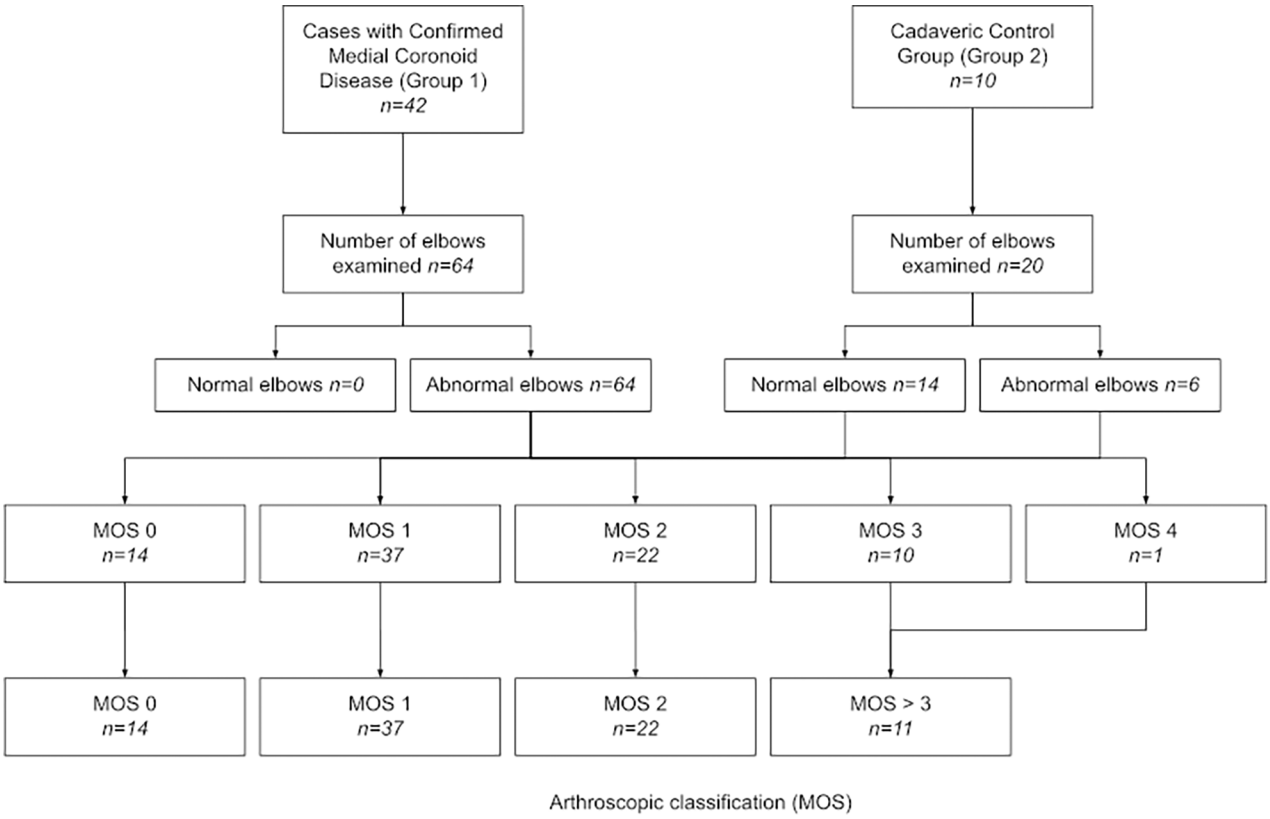

Figure 2—Flow diagram outlining case recruitment for groups 1 and 2, and the final classification of included elbow joints by arthroscopic disease classification (Modified Outerbridge score [MOS]).

followed by contemporaneous arthroscopic examination. Dogs were between 6 months and 8 years 11 months. From these dogs, 64 elbow joints were assessed (22 cases with bilateral MCD and 20 cases with unilateral MCD). This group consisted of dogs weighing between 11.4 and 52 kg (mean, 31.05 kg). The data were normally distributed. Elbow joints examined in group 1 were from the following breeds: Labrador Retriever (n = 31), German Shepherd Dog (n = 6), Rottweiler (n = 6), cross-breed (n = 4), Boxer (n = 4), Bulldog (n = 3), English Springer Spaniel (n = 3), Cavalier King Charles Spaniel (n = 2), Bull Mastiff (n = 2), Cocker Spaniel (n = 2), and Labradoodle (n = 1).

After arthroscopic examination of the cadaveric control group, an additional 6 elbow joints from 5 dogs had evidence of MCD (1 case with bilateral MCD and 4 cases with unilateral MCD) and were moved to group 1, resulting in a total of 70 elbow joints examined in group 1. Prior medical history of these patients was unknown, but all were Staffordshire Bull Terriers (n = 6), skeletally mature and weighed between 18 and 30 kg.

Of 70 elbow joints, 37 had a MOS = 1, 22 had a MOS = 2, 10 had a MOS = 3, and 1 had a MOS = 4. No animals were examined with a MOS > 4. Because only a single case was examined with a MOS of 4, this case was pooled with those with a MOS ≥ 3 for final statistical analysis (Figure 2).

Group 2: cases with no evidence of MCD (MOS = 0)

The remaining (control) group of cadaveric animals consisted of 9 animals, with an assessment of 14 elbow joints. Prior medical history of these patients was unknown and dogs weighed between 18 and 30 kg (mean, 20.4 kg). All of these patients were skeletally mature. Elbow joints examined in group 2 were from the following breeds: Staffordshire Bull Terrier or Staffordshire Bull Terrier Crosses (n = 14). All 14 elbow joints in this group had a MOS = 0 (Figure 2).

Relationship between the attenuation of the MCP and PRC in dogs with and without arthroscopic evidence of MCD

The mean attenuation of the MCP and PRC across all arthroscopic grading categories were 1,361.94 HU and 1,581.73 HU, respectively. The data were normally distributed and the paired *t* test suggested that the overall attenuation of the PRC across all grading categories was significantly greater than the overall attenuation of the MCP ($P < .001$).

Relationship between the attenuation of the MCP in dogs with and without MCD

The distribution of the mean attenuation of the MCP in dogs with and without arthroscopic cartilage

lesions is outlined in **Table 2** and summarized in **Figure 3**. The data were normally distributed.

Multilevel linear regression analysis confirmed a significant relationship ($P < .002$) between the attenuation of the MCP in dogs with and without arthroscopic cartilage lesions. A significantly greater attenuation of the MCP in dogs scoring 0 at arthroscopy was noted compared with dogs that had MOS = 1, 2, or 3 ($P < .002$). However, no significant differences in attenuation were noted between the different severity categories of arthroscopically diseased elbow joints.

Table 2—Mean attenuation of the medial coronoid process (MCP) and mean attenuation of the MCP normalized to the proximal radial cortex across the arthroscopic grading category.

MOS	Mean attenuation of the MCP (HU)	Mean attenuation of the MCP normalized to the PRC (HU/HU)
0 (n = 14)	1,606.56(Ref)	0.86
1 (n = 37)	1,302.16*	0.89
2 (n = 22)	1,350.31*	0.83
≥ 3 (n = 11)	1,274.97*	0.86

HU = Hounsfield unit; MOS = Modified Outerbridge score; PRC = Proximal radial cortex.

*$P < .002$, significance from reference (MOS = 0).

Relationship of the MCP normalized to PRC in dogs with and without MCD

The distribution of the mean attenuation of the MCP normalized to the PRC (MCP/PRC, measured in Hounsfield units) in dogs with and without arthroscopic cartilage lesions is outlined in Table 2 and summarized in **Figure 4**. The data were normally distributed.

Multilevel linear regression analysis confirmed no statistically significant relationships between the mean attenuation of the MCP and arthroscopic categories when normalized to the mean attenuation of the PRC ($P = .68$).

Inter- and intraobserver variability

There was good interobserver reliability (ICC, 0.89; 95% CI, 0.66 to 0.95; $P < .05$) between the measurements of the attenuation obtained by observer 1 and observer 2. There was excellent intraobserver reliability (ICC, 0.95; 95% CI, 0.87 to 0.97; $P < .001$) between measurements taken by observer 2.

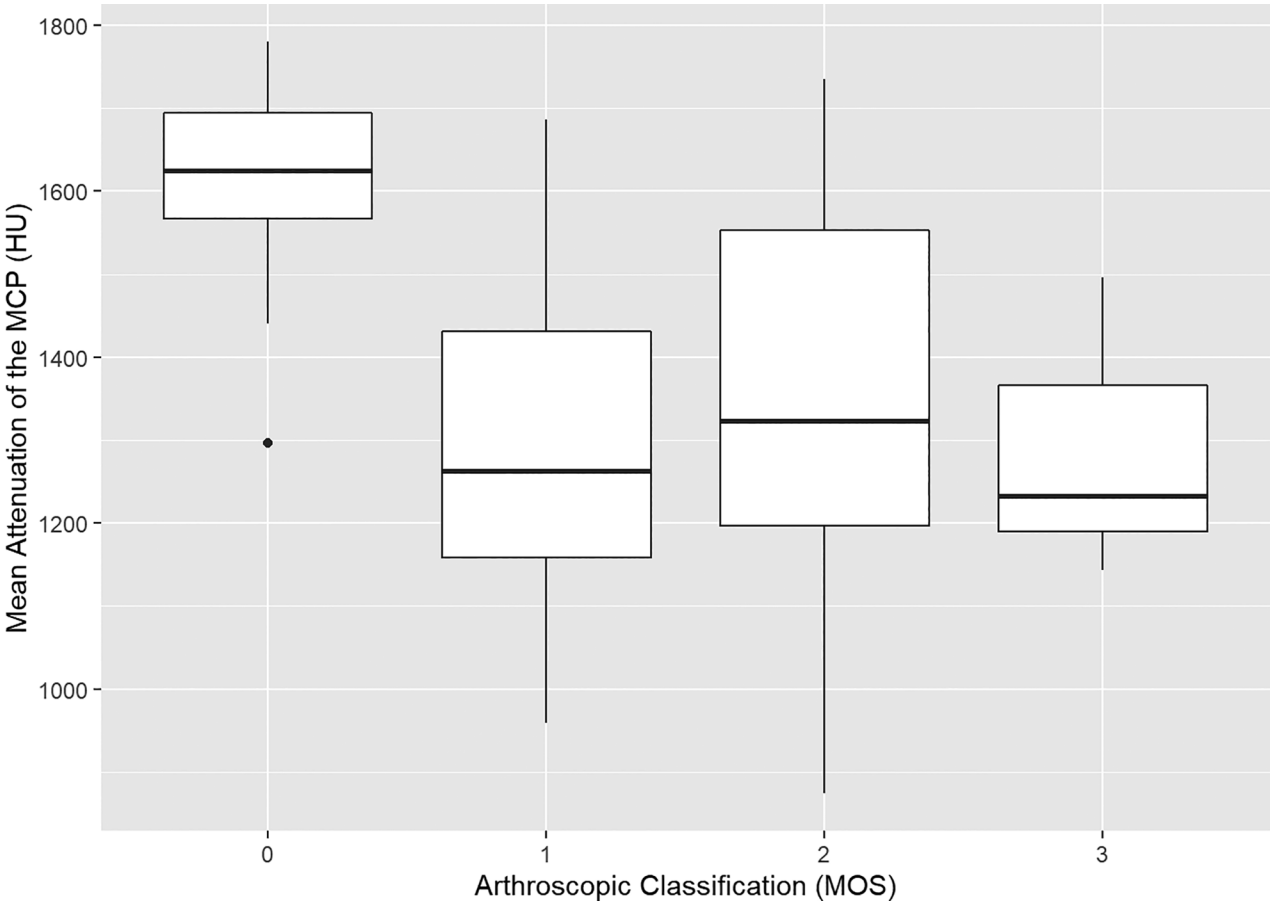

Figure 3—Box-and-whisker plot showing attenuation of the medial coronoid process (MCP) (measured in Hounsfield units) within and between categories of arthroscopic disease severity. MOS = Modified Outerbridge score.

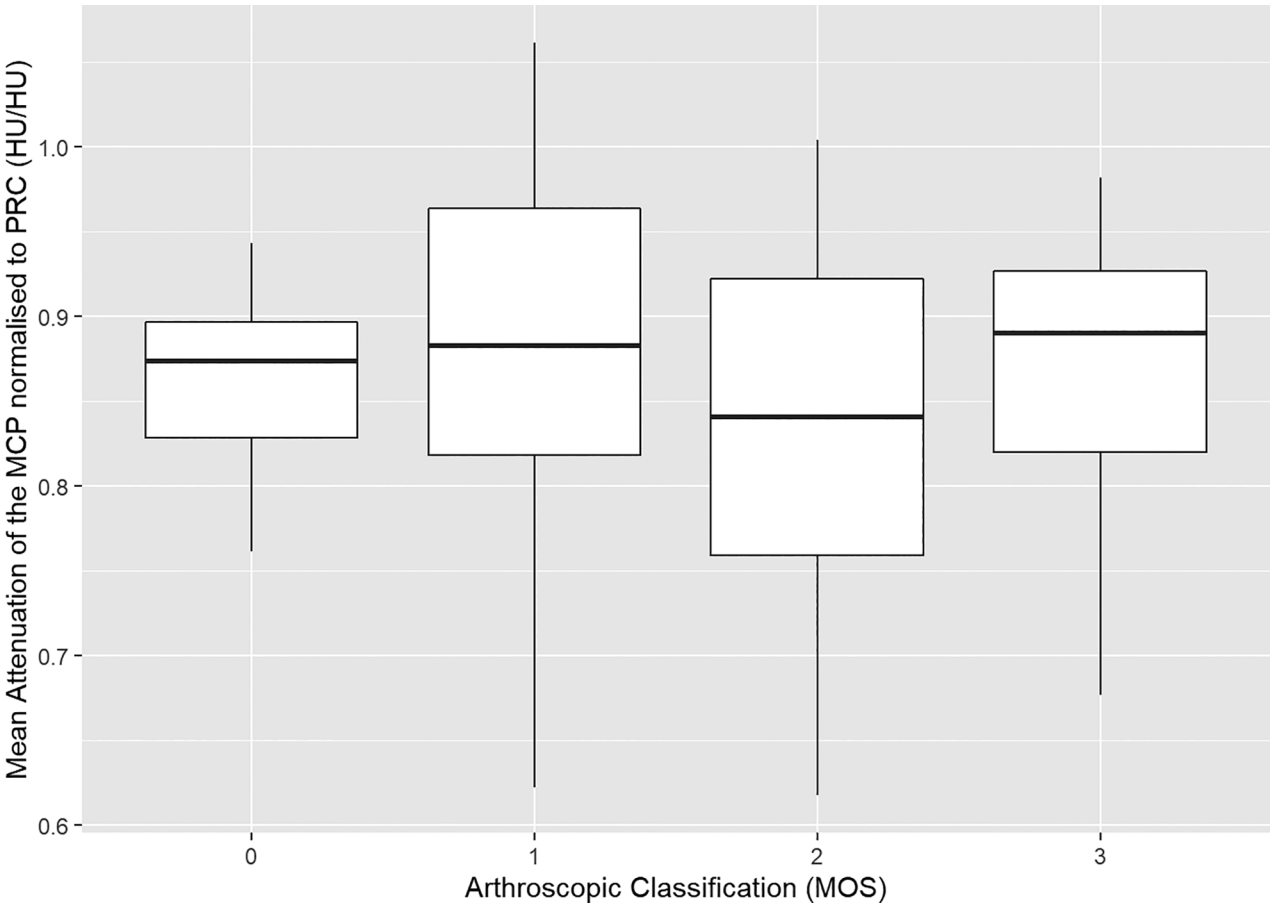

Figure 4—Box-and-whisker plot showing attenuation of the medial coronoid process (MCP) normalized to the attenuation of the proximal radial cortex (PRC) (measured in Hounsfield units/Hounsfield units) within and between categories of arthroscopic disease severity. MOS = Modified Outerbridge score.

Discussion

The results of this study led us to reject our null hypothesis, concluding there was a significantly lower attenuation in the MCP and PRC in dogs with MCD compared with dogs without evidence of MCD upon arthroscopic examination of the elbow joint.

Bone is a dynamic tissue, responding to mechanical load via Wolff's law.[33] Accordingly, under normal physiologic conditions, reduction in BMD and therefore attenuation may reflect altered load within the osseous structures of the elbow joint. Phillips et al[6] postulate a caudolateral load transfer within affected thoracic limbs as the physiologic mechanism underlying the reduction in overall attenuation of the MCP in dogs with MCD, a theory supported by the results of our study and the findings of the recent work by Wennemuth et al.[34] We additionally found a parallel reduction in attenuation within the PRC, a finding supported by that of Villamonte-Chevalier et al[28] in their population of Golden and Labrador Retrievers. This finding might further support the theory proposed by Phillips et al,[6] given the roughly equal load sharing of the radius and ulna reported with in vitro force plate analysis in the canine elbow joint by Mason et al.[35] A caudolateral load shift through the ulna could reasonably be expected also to unload the radius to a degree significant enough to result in reduced BMD. Alternatively, the hypoattenuation observed in our study might reflect an overall reduction in load on a thoracic limb unilaterally with contralateral weight shift, as might be expected with a degree of disuse osteopenia.[36] However, this would require measurements of attenuation from additional distant locations not taken in our study and/or measurements from a population of dogs with true unilateral disease verified with force plate data.

Despite there being a significantly lower attenuation of the MCP and PRC in cases from our study with arthroscopic evidence of MCD, no significant relationship was shown for increasing severity categories of cartilage damage (MOS). This finding supports the results of a previous study in which imaging and arthroscopic evidence of disease were not correlative with clinical presentation.[37] Our results suggest that reduced or altered load within a diseased elbow joint occurs consistently and repeatedly, but independent of actual arthroscopic disease severity. A clinical presentation score was not used in our study, and therefore association between clinical presentation and attenuation of the MCP could not be assessed. The reduction in attenuation independent

of arthroscopic severity might support the adjunctive use of CT attenuation for early detection of reduced load bearing secondary to MCD, and the good inter- and intraobserver variability reported earlier demonstrates consistency in the technique described. However, it is clear from the literature that numerous factors, including age, breed, and disease course, affect the attenuation of the MCP; therefore, continued research is warranted in this area.[6,38]

There were several limitations to our study. A number of studies[6,8,28,39] have reported variation in the bone density of the microstructure of the MCP in sagittal planes or zones. Although standardized, our measurement of the MCP consisted of a polygon drawn around the entire MCP from the apex to the base on a single slice, providing a general overview of the attenuation but potentially limiting insight into the variation in attenuation between zones of the MCP itself. Villamonte-Chevalier et al[28] reported that the most consistent results were found when using the MCP base to make an assessment of the attenuation of the MCP, and further work should continue to optimize consistent and repeatable measurement locations for the MCP. This is of particular relevance given the presence of fissures (without overt fragmentation) through the MCP, which could conceivably reduce the attenuation when included within a region of measurement. It is also possible that variation in attenuation might occur between the MCP on adjacent slices and that assessment on a single slice might not have provided a representative measurement of the overall attenuation of the MCP. Last, CT has been shown to provide variable consistency in measurement of the attenuation of trabecular bone (up to 5% to 8%), and reduction of this value to ~3% can be achieved with CTOAM and the use of a dipotassium phosphate standardization device.[40] Although we believe this is unlikely to have affected the results of this study significantly, it is potential consideration for future work in this area.

There were further limitations inherent within the study population. First, the comparison of performing CT scans on cadavers with elbow joints scanned in vivo during clinical investigation may draw criticism. However, scanning frozen limbs postmortem has been shown to have no effect on the overall attenuation of trabecular bone identified by CT.[40] We believe the benefit of contemporaneous arthroscopic examination for confirmation of disease status in normal animals (group 2) outweighs any negative impact of postmortem examination allowing accurate comparison of attenuation without subjecting a population of normal dogs to unjustified (in vivo) arthroscopic examination.[40] Although the reliability of the MOS has been challenged in human arthroscopy, the intra- and interobserver reliability is reportedly high in canine patients, particularly in observers with extensive experience.[41] Second, the overrepresentation of the Labrador Retriever breed in group 1 is a potential confounding factor. Phillips et al[6] reported a significant difference in the attenuation of the MCP between a population of Greyhounds and Labrador Retrievers, suggesting significant interbreed variation in attenuation of the MCP. Ideally, breed matched case–controls would negate this bias, but this consideration was not practical for this study. Last, the lack of age data for group 2 is a potential limitation on conclusions from this study population. Dickomeit et al[38] reported an age-dependent increase in subchondral bone density via CTOAM. It is possible that some degree of the parallel increase in attenuation of the MCP and PRC is a result of normal aging change, should a number of the cases in group 2 be significantly older than those in group 1. However, we believe that group 1 was sufficiently heterogeneous with regard to age to negate this hypothesis.

To conclude, we have reported a significantly lower attenuation in the MCP and PRC in dogs with evidence of MCD at elbow arthroscopy. CED is a complex multifactorial disease and it is clear that the attenuation pattern and BMD change dynamically throughout the disease course as a result of altered microstress/strain placed on the elbow joint. CT provides a noninvasive method to assess the attenuation of the bony structures of the elbow joint throughout the disease course. However, further research into the temporal changes in attenuation in individual cases followed longitudinally and among breeds is warranted before routine clinical implementation of this technique.

Acknowledgments

No third-party funding or support was received in connection with this study or the writing or publication of this manuscript.

The authors declare that there were no conflicts of interest.

We acknowledge Ben Jones and Lee Moore at the Veterinary Teaching Suite for their assistance with the cadaveric samples.

References

1. International Elbow Working Group. International Elbow Working Group. 2020. Accessed April 15, 2020. http://www.vet-iewg.org/
2. Cook CR, Cook JL. Diagnostic imaging of canine elbow dysplasia: a review. *Vet Surg.* 2009;38(2):144–153. doi:10.1111/j.1532-950X.2008.00481.x
3. Kirberger RM, Fourie SL. Elbow dysplasia in the dog: pathophysiology, diagnosis and control. *J South Afr Vet Assoc.* 1998;69(2):43–54. doi:10.4102/jsava.v69i2.814
4. Michelsen J. Canine elbow dysplasia: aetiopathogenesis and current treatment recommendations. *Vet J.* 2013;196(1):12–19. doi:10.1016/j.tvjl.2012.11.009
5. Samii VF, Les CM, Schulz KS, Keyak JH, Stover SM. Computed tomographic osteoabsorptiometry of the elbow joint in clinically normal dogs. *Am J Vet Res.* 2002;63(8):1159–1166. doi:10.2460/ajvr.2002.63.1159
6. Phillips A, Burton NJ, Warren-Smith CMR, Kulendra ER, Parsons KJ. Topographic bone density of the radius and ulna in Greyhounds and Labrador Retrievers with and without medial coronoid process disease. *Vet Surg.* 2015;44(2):180–190. doi:10.1111/j.1532-950X.2014.12294.x
7. Mostafa A, Nolte I, Wefstaedt P. The prevalence of medial coronoid process disease is high in lame large breed dogs and quantitative radiographic assessments contribute

to the diagnosis. *Vet Radiol Ultrasound.* 2018;59(5): 516–528. doi:10.1111/vru.12632
8. Burton NJ, Perry MJ, Fitzpatrick N, Owen MR. Comparison of bone mineral density in medial coronoid processes of dogs with and without medial coronoid process fragmentation. *Am J Vet Res.* 2010;71(1):41–46. doi:10.2460/ajvr.71.1.41
9. Nemanic S, Nixon BK, Baltzer W. Analysis of risk factors for elbow dysplasia in giant breed dogs. *Vet Comp Orthop Traumatol.* 2016;29(5):369–377. doi:10.3415/VCOT-15-05-0175
10. Hans EC, Saunders WB, Beale BS, Hulse DA. Fragmentation of the medial coronoid process in toy and small breed dogs: 13 elbows (2000–2012). *J Am Anim Hosp Assoc.* 2016;52(4):234–241. doi:10.5326/JAAHA-MS-6295
11. Moores AP, Benigni L, Lamb CR. Computed tomography versus arthroscopy for detection of canine elbow dysplasia lesions. *Vet Surg.* 2008;37(4):390–398. doi:10.1111/j.1532-950X.2008.00393.x
12. Van Ryssen B, Van Bree H. Arthroscopic findings in 100 dogs with elbow lameness. *Vet Rec.* 1997;140(14): 360–362. doi:10.1136/vr.140.14.360
13. Fitzpatrick N, Yeadon R. Working algorithm for treatment decision making for developmental disease of the medial compartment of the elbow in dogs. *Vet Surg.* 2009;38(2): 285–300. doi:10.1111/j.1532-950X.2008.00495.x
14. Proks P, Necas A, Stehlik L, Srnec R, Griffon DJ. Quantification of humeroulnar incongruity in Labrador Retrievers with and without medial coronoid disease. *Vet Surg.* 2011;40(8): 981–986. doi:10.1111/j.1532-950X.2011.00907.x
15. Preston CA, Schulz KS, Kass PH. In vitro determination of contact areas in the normal elbow joint of dogs. *Am J Vet Res.* 2000;61(10):1315–1321. doi:10.2460/ajvr.2000.61.1315
16. Hulse D, Young B, Beale B, Kowaleski M, Vannini R. Relationship of the biceps–brachialis complex to the medial coronoid process of the canine ulna. *Vet Comp Orthop Traumatol.* 2010;23(3):173–176. doi:10.3415/VCOT-09-06-0063
17. Burton NJ, Warren-Smith CMR, Roper DP, Parsons KJ. CT assessment of the influence of dynamic loading on physiological incongruency of the canine elbow. *J Small Anim Pract.* 2013;54(6):291–298. doi:10.1111/jsap.12093
18. Lau SF, Wolschrijn CF, Siebelt M, Vernooij JCM, Voorhout G, Hazewinkel HAW. Assessment of articular cartilage and subchondral bone using EPIC-microCT in Labrador Retrievers with incipient medial coronoid disease. *Vet J.* 2013;198(1):116–121. doi:10.1016/j.tvjl.2013.05.038
19. Wavreille V, Fitzpatrick N, Drost WT, Russell D, Allen MJ. Correlation between histopathologic, arthroscopic, and magnetic resonance imaging findings in dogs with medial coronoid disease. *Vet Surg.* 2014;44(4):501–510. doi:10.1111/j.1532-950X.2014.12233.x
20. Fitzpatrick N, Garcia TC, Daryani A, Bertran J, Watari S, Hayashi K. Micro-CT structural analysis of the canine medial coronoid disease. *Vet Surg.* 2016;45(3):336–346. doi:10.1111/vsu.12449
21. Gemmill TJ, Hammond G, Mellor D, Sullivan M, Bennett D, Carmichael S. Use of reconstructed computed tomography for the assessment of joint spaces in the canine elbow. *J Small Anim Pract.* 2006;47(2):66–74. doi:10.1111/j.1748-5827.2006.00052.x
22. Villamonte-Chevalier A, van Bree H, Broeckx B, et al. Assessment of medial coronoid disease in 180 canine lame elbow joints: a sensitivity and specificity comparison of radiographic, computed tomographic and arthroscopic findings. *BMC Vet Res.* 2015;11:243. doi:10.1186/s12917-015-0556-9
23. Wagner K, Griffon DJ, Thomas MW, et al. Radiographic, computed tomographic, and arthroscopic evaluation of experimental radio-ulnar incongruence in the dog. *Vet Surg.* 2007;36(7):691–698. doi:10.1111/j.1532-950X.2007.00322.x
24. Griffon DJ, Mostafa AA, Blond L, Schaeffer DJ. Radiographic, computed tomographic, and arthroscopic diagnosis of radioulnar incongruence in dogs with medial coronoid disease. *Vet Surg.* 2018;47(3):333–342. doi:10.1111/vsu.12783
25. Kramer A, Holsworth IG, Wisner ER, Kass PH, Schulz KS. Computed tomographic evaluation of canine radioulnar incongruence in vivo. *Vet Surg.* 2006;35(1):24–29. doi:10.1111/j.1532-950X.2005.00107.x
26. Snaps FR, Balligand MH, Saunders JH, Park RD, Dondelinger RF. Comparison of radiography, magnetic resonance imaging, and surgical findings in dogs with elbow dysplasia. *Am J Vet Res.* 1997;58(12):1367–1370.
27. Franklin SP, Burke EE, Holmes SP. Utility of MRI for characterizing articular cartilage pathology in dogs with medial coronoid process disease. *Front Vet Sci.* 2017;4(4):25. doi:10.3389/fvets.2017.00025
28. Villamonte-Chevalier A, Dingemanse W, Broeckx BJG, et al. Bone density of elbow joints in Labrador Retrievers and Golden Retrievers: comparison of healthy joints and joints with medial coronoid disease. *Vet J.* 2016;216:1–7. doi:10.1016/j.tvjl.2016.06.005
29. d'Anjou M-A. Principles of computed tomography and magnetic resonance imaging. In: Thrall DE, ed. *Textbook of Veterinary Diagnostic Radiology.* 7th ed. Saunders; 2018;71–95. doi:10.1016/B978-0-323-48247-9.00017-6
30. Rosset A, Spadola L, Ratib O. OsiriX: an open-source software for navigating in multidimensional DICOM images. *J Digit Imaging.* 2004;17(3):205–216. doi:10.1007/s10278-004-1014-6
31. Beale B, Hulse D, Schulz K, Whitney W. *Small Animal Arthroscopy.* 1st ed. Saunders; 2003.
32. Koo TK, Li MY. A guideline of selecting and reporting intraclass correlation coefficients for reliability research. *J Chiropr Med.* 2016;15(2):155–163. doi:10.1016/j.jcm.2016.02.012
33. Barak MM, Lieberman DE, Hublin JJ. A Wolff in sheep's clothing: trabecular bone adaptation in response to changes in joint loading orientation. *Bone.* 2011;49(6): 1141–1151. doi:10.1016/j.bone.2011.08.020
34. Wennemuth J, Tellhelm B, Eley N, Von Pückler K. Computed tomography enhances diagnostic accuracy in challenging medial coronoid disease cases: an imaging study in dog breeding appeal cases. *Vet Comp Orthop Traumatol.* 2020;33(5):356–362. doi:10.1055/s-0040-1714299
35. Mason DR, Schulz KS, Fujita Y, Kass PH, Stover SM. In vitro force mapping of normal canine humeroradial and humeroulnar joints. *Am J Vet Res.* 2005;66(1):132–135. doi:10.2460/ajvr.2005.66.132
36. Schreiber JJ, Anderson PA, Rosas HG, Buchholz AL, Au AG. Hounsfield units for assessing bone mineral density and strength: a tool for osteoporosis management. *J Bone Joint Surg A.* 2011;93(11):1057–1063. doi:10.2106/JBJS.J.00160
37. Fitzpatrick N, Smith TJ, Evans RB, Yeadon R. Radiographic and arthroscopic findings in the elbow joints of 263 dogs with medial coronoid disease. *Vet Surg.* 2009;38(2): 213–223. doi:10.1111/j.1532-950X.2008.00489.x
38. Dickomeit MJ, Böttcher P, Hecht S, Liebich HG, Maierl J. Topographic and age-dependent distribution of subchondral bone density in the elbow joints of clinically normal dogs. *Am J Vet Res.* 2011;72(4):491–499. doi:10.2460/ajvr.72.4.491
39. Danielson KC, Fitzpatrick N, Muir P, Manley PA. Histomorphometry of fragmented medial coronoid process in dogs: a comparison of affected and normal coronoid processes. *Vet Surg.* 2006;35(6):501–509. doi:10.1111/j.1532-950X.2006.00183.x
40. Cann CE. Quantitative CT for determination of bone mineral density: a review. *Radiology.* 1988;166(2):509–522. doi:10.1148/radiology.166.2.3275985
41. Deweese M, Brown D, Hayashi K, et al. Observer variability of arthroscopic cartilage grading using the modified Outerbridge classification system in the dog. *Vet Comp Orthop Traumatol.* 2019;32(2):126–132. doi:10.1055/S-0039-1678550